Research Article

Moorthy Muruganandham, Fatimah Oleyan Al-Otibi, Raedah Ibrahim Alharbi, Kanagasabapathy Sivasubramanian, Ramalingam Karthik Raja, Palanivel Velmurugan*, and Nagaraj Basavegowda*

Antibacterial, antifungal, antioxidant, and cytotoxicity activities of the *aqueous* extract of *Syzygium aromaticum*-mediated synthesized novel silver nanoparticles

https://doi.org/10.1515/gps-2023-0188 received July 27, 2023; accepted November 7, 2023

Abstract: The synthesis of silver nanoparticles using plantbased materials has seen a surge in recent years. This study used the Syzygium aromaticum (clove) buds extract as a reducing agent for synthesizing silver nanoparticles (Sa-AgNPs). The presence of Sa-AgNPs (440 nm) was confirmed by UV-Vis spectroscopy. The optimization of nanoparticle production with pH, metal ions, and substrate concentration (clove extract) was studied. The transmission electron microscopy analysis revealed that Sa-AgNPs had a size distribution predominantly below the range of 10-100 nm. The investigation of Sa-AgNPs using EDX revealed the presence of an optical absorption silver peak at 3 keV. The involvement of phenolic chemicals and carboxylic acids in stretching O-H, N-O, and C=O bonds, forming Sa-AgNPs has been identified by Fourier transform infrared spectroscopy. Klebsiella pneumoniae and Trichophyton rubrum exhibited a higher inhibition zone of 26 \pm 0.48 mm and 21 \pm 0.48 mm in antibacterial and antifungal activity, respectively. In the 2,2-diphenyl-1-picrylhydrazyl experiment, at a maximum concentration of 500 $\mu g \cdot m L^{-1}$, Sa-AgNPs exhibited a scavenging efficiency of 79.98%. Cytotoxicity was observed in the treated cells due to the presence of biologically synthesized Sa-AgNPs. An IC_{50} value of 48 $\mu g \cdot m L^{-1}$ was determined by treating L929 human fibroblast cells.

Keywords: S. aromaticum, Sa-AgNPs, TEM, FT-IR, MTT assay

1 Introduction

Nanoparticles reveal atom-like characteristics due to their increased energy distribution on the surface, which arises from their substantial and expansive specific surface area, a significant proportion of surface atoms, and the substantial disparity between the valence and conduction band when reduced to sizes approaching atomic dimensions [1,2]. The earlier-mentioned characteristic has attracted significant interest among researchers seeking to develop innovative production approaches. Compared to the early half of the century, recent decades have seen a lightning-fast acceleration in nanoparticle synthesis. Physicochemical techniques were previously employed to synthesize nanoparticles [3]. Chemical and physical nanoparticle synthesis methods require hazardous substances, necessitate significant energy consumption, and generate plenty of waste. In response to these challenges, "green synthesis" techniques are a promising technology in nanoparticle synthesis. Green synthesis uses plant extracts, microbes, and proteins to reduce and stabilize metal ions for nanoparticle production. The benefits of green nanoparticle synthesis include energy efficiency, biocompatibility, and personalized functions [4,5]. This is because plant extract-mediated nanoparticle production

Moorthy Muruganandham, Kanagasabapathy Sivasubramanian: Centre for Materials Engineering and Regenerative Medicine, Bharath Institute of Higher Education and Research, Selaiyur, Chennai-73, Tamil Nadu, India

Fatimah Oleyan Al-Otibi, Raedah Ibrahim Alharbi: Department of Botany and Microbiology, College of Science, King Saud University, P.O. Box 22452, Riyadh 11451, Saudi Arabia

Ramalingam Karthik Raja: Department of Research and Innovation, Saveetha School of Engineering, Saveetha Institute of Medical and Technical Sciences (SIMATS), Chennai 602105, Tamil Nadu, India

^{*} Corresponding author: Palanivel Velmurugan, Centre for Materials Engineering and Regenerative Medicine, Bharath Institute of Higher Education and Research, Selaiyur, Chennai-73, Tamil Nadu, India, e-mail: palanivelmurugan2008@gmail.com

^{*} Corresponding author: Nagaraj Basavegowda, Department of Biotechnology, Yeungnam University, Gyeongsan, Gyeongbuk 38451, Korea, e-mail: nagarajb2005@yahoo.co.in

is inexpensive. The high ratio of surface area to volume exhibited by nanoparticles is a prominent characteristic that facilitates strong molecular interactions due to their smaller size, distribution, and morphology [6]. The utilization of green synthesis methods for the production of nanoparticles offers numerous advantages, including environmental sustainability, reduced time requirements, cost-effectiveness, operational stability, and, most notably, the absence of hazardous chemical involvement [7,8].

The significance of noble AgNPs in various scientific and technological domains, including medicine, cannot be ignored due to their origin. Therefore, it is imperative to prioritize the exploration of an alternative synthetic route that is not only cost-effective but also environmentally friendly. Considering the aesthetic conditions, the use of green syntheses is emerging as a prominent procedure, showcasing its significant potential [9]. Physical, chemical, and biological methods are used to synthesize nanoparticles. Physical procedures like laser ablation and ball milling and chemical approaches like chemical reduction and sol-gel technologies have dominated this field. These methods have made great strides, but they use a lot of energy, chemicals, and waste. Nanoparticle size and form are difficult to regulate. The more sustainable option is biological synthesis, often known as green synthesis. These approaches use plant extracts, microbes, and biomolecules to reduce and cap. Natural resources decrease the need for harsh chemicals and extreme conditions and improve biocompatibility and environmental impact. Biological synthesis allows for the creation of nanoparticles with well-defined properties for specific purposes. This method follows green chemistry and offers a sustainable nanoparticle production option [10].

This study aims to investigate the broad potential of plants as feasible sources for the synthesis of AgNPs, utilizing a biological green technique as a counterpart to standard methods. The extract of S. aromaticum, commonly referred to as clove, which belongs to the Myrtaceae family, was employed for the biosynthesis of silver ions into nanoparticles. Based on the chemical composition analysis, it can be inferred that the clove essential oil exhibits promising characteristics as a silver-reducing agent in the synthesis of nanoparticles. The reduction process can be attributed to the proton donation from the eugenol structure. This proton donation results in the reduction of Ag+ to Ag0, thereby promoting the formation of nanoparticles. The hypothesis behind this study reveals that using the S. aromaticum (clove) aqueous extract to synthesize AgNPs with well-defined size, shape, and surface characteristics is sustainable and eco-friendly. Bioactive components in the extract, particularly phenolic compounds, and terpenoids, may reduce silver ions and stabilize nanoparticles as reducing and capping agents. This green synthesis method is projected to produce AgNPs with improved biocompatibility, stability, and antibacterial and antioxidant capabilities, promising biomedical and environmental applications.

Furthermore, it has been observed that the phytochemicals found in the essential oil exhibit the ability to interact with the surface of nanoparticles. This interaction significantly enhances the stability and maintenance of the nanoparticles [11,12]. AgNPs can be synthesized at a reduced concentration of the clove extract, preventing the need for supplementary chemical or physical techniques that may pose potential harm. The effect of the amount of clove extract and metal ions on the production of AgNPs in order to improve the process was also studied. The study's methodology stands out for its simplicity, cost-effectiveness, ease of implementation, and long-term sustainability.

2 Materials and methods

2.1 Materials

S. aromaticum buds were procured from the local market in Chennai, India. The chemicals and solvents utilized in this study were of analytical grade: silver nitrate (AgNO₃) (99.9%) and 2,2-diphenyl-1-picrylhydrazyl (DPPH) (95%) were obtained from SRL, India. 3-(4,5-Dimethylthiazol-2yl)-2,5-diphenyl tetrazolium bromide (MTT) (98%) and the Mueller Hinton agar (MHA) medium were obtained from Hi-Media, Mumbai, India. The laboratory-acquired tetracycline from Hi-Media (Mumbai, India) was used as a reference antibiotic with a minimum potency of 720 IU·mg⁻¹. Double distilled water (dDW) was used to prepare all aqueous solutions during the study.

2.2 Preparation of the aqueous extract

In the initial step, a precise quantity of 1 g of finely powdered *S. aromaticum* buds was added to 100 mL of dDW. The mixture was then boiled at 100°C for 30 min to obtain the aqueous extract. After cooling at room temperature, the extract was filtered using Whatman No. 1 filter paper. Subsequently, it was stored at a temperature of 4°C to facilitate subsequent experimental investigations.

2.3 Biosynthesis of AgNPs

A solution of Ag^+ ion at a concentration of $0.1\,\text{mM}$ was employed in the biosynthesis of AgNPs. About $1\,\text{mL}$ of the

S. aromaticum aqueous extract was mixed with 9 mL of 0.1 mM AgNO₃ solution. The mixture was thoroughly mixed at room temperature. The resultant mixture was left undisturbed in a dark place. After a few hours, the color of the solution changed from light brown to dark brown due to the formation of Sa-AgNPs. This change was periodically monitored by measuring the absorbance of the solution UV-visible spectroscopy in the wavelength range of 200–800 nm.

2.4 Optimization of Sa-AgNP synthesis

Optimization of nanoparticles was carried out using different pH values, metal ions concentrations (AgNO₃), and substrate concentrations (S. aromaticum aqueous extract). About 1.0 mL of the S. aromaticum aqueous extract and 9.0 mL of a 0.1 mM AgNO₃ solution were mixed. The resultant mixture was then monitored for any development in color, specifically a change to dark brown, under different pH conditions ranging from 3 to 11. The pH levels were maintained at room temperature throughout the observation period. For metal ions, a concentration of 1.0 mL volume of the S. aromaticum aqueous extract was mixed with 9.0 mL of AgNO₃ solution at various concentrations (100, 200, 300, 400, and 500 mM) at a pH of 8.0. The mixture was then incubated at room temperature. To improve the production of Sa-AgNPs, different volumes of the S. aromaticum aqueous extract (0.5, 1, 1.5, 2, and 2.5 mL) were employed at room temperature. These volumes were then adjusted to a final volume of 10 mL using a 0.1 mM AgNO₃ solution at a pH of 8.0. The absorbance of the resultant mixture was measured using a UV-Vis spectrophotometer (UV-1800, Genesys 180, Thermo Fisher Scientific, USA) in the 300-800 nm wavelength range.

2.5 Synthesis of AgNPs

The synthesis of AgNPs was successfully achieved by adjusting the pH, substrate, and AgNO $_3$ concentrations. After mass production, the solution containing AgNPs was subjected to numerous cycles of centrifugation at a speed of 9,660×g for 30 min. The pellet was subjected to freeze-drying for further analysis.

2.6 Characterization of Sa-AgNPs

A distinct alteration in color, explicitly transitioning from a light brown to a dark brown color, was noted in the AgNO₃

solution after incubating with an aqueous extract. To effectively monitor the bioreduction process of Ag nanoparticles, the absorbance and spectrum of the solution were consistently measured using a UV spectrophotometer (UV-1800, Genesys 180, Thermo Fisher Scientific, USA) in the wavelength range of 300-800 nm. The particle size, shape, and particle size distributions were determined using transmission electron microscopy (TEM) with a JEOL JEM-2011 microscope (Tokyo, Japan) operating at an accelerating voltage of 200 kV. To facilitate the preparation of samples for TEM analysis, a small volume of the solution was carefully deposited onto a copper grid coated with a layer of carbon. Subsequently, the grid was left undisturbed for natural ambient air drying. The elemental composition of the synthesized Sa-AgNPs was determined by analyzing the EDX spectrum, to examine the energy dispersal [13]. X-ray diffraction (XRD) patterns facilitated the examination of the crystalline nature of the synthesized Sa-AgNPs using the aqueous extract of S. aromaticum. XRD analysis was conducted to determine the crystalline properties, size, and phase identification of the Sa-AgNPs. Fourier transform infrared (FTIR) spectroscopy is a powerful analytical technique to elucidate the functional groups in the synthesized Sa-AgNPs. It is widely recognized for its ability to provide valuable information about various materials' chemical composition and molecular structure. The synthesized Sa-AgNPs functional groups were analyzed using FTIR spectroscopy (Nicolet Summit LITE FTIR spectrometer manufactured by Thermo Fisher Scientific, USA) by obtaining the FTIR spectrum in the wavelength range of 4,000-500 cm⁻¹ [14].

2.7 Biomedical applications

2.7.1 Well diffusion method

The agar well diffusion technique was used to evaluate the antibacterial efficacy of the synthesized AgNPs. The bacterial strains, including *Enterococcus faecalis, Staphylococcus aureus, Klebsiella pneumonia, Proteus mirabilis,* and *Pseudomonas aeruginosa,* were subjected to subculturing in the Muller–Hinton broth (MHB) medium. The subcultures were then incubated at 37°C for 24 h. The overnight cultures that were acquired were swabbed onto Muller–Hinton agar plates to promote the development of a consistent microbial colony. Each Petri plate containing the microbial culture was subjected to a well cut with a uniform diameter to inoculate the Sa-AgNPs, extract and control, and each sample was prepared at 5 mg·mL⁻¹. Sa-AgNPs were dissolved in dimethylsulfoxide (DMSO). The investigation of the antibacterial activity involved the inclusion of AgNPs,

aqueous extract, and the antibiotic tetracycline as the control group. Following that, the Petri dishes were subjected to a 24 h incubation period at a temperature of 37°C. Similarly, antifungal efficacy was evaluated using fungal strains, including Aspergillus fumigatus, Candida albicans, Mucor sp. Trichophyton rubrum, and Epidermophyton floccosum. They were subjected to subculturing in potato dextrose broth, and the subcultures were subsequently subjected to incubation at 28°C for 48 h. The acquired fungal spores were inoculated onto potato dextrose agar plates to facilitate the growth of a uniform microbial colony. The study on antifungal activity encompassed the incorporation of Sa-AgNPs, aqueous extract, and nvstatin as the control. Subsequently, the Petri dishes were incubated for 48 h at a temperature of 28°C. To assess how well the synthesized silver nanoparticles work as an antibacterial agent, the diameter of the zone of inhibition was measured and subsequently compared to that of the control groups [14].

2.7.2 Determination of the minimum inhibition concentration (MIC)

To ascertain the MIC, a consistent inoculum of spores at a concentration of 1×10^7 colony-forming units per milliliter (CFU·mL⁻¹) was combined with the MHB. Subsequently, various concentrations of an aqueous extract ranging from 1.56 to $100~\mu g \cdot mL^{-1}$ were added, along with tetracycline as a standard drug. Subsequently, the broths were incubated under aseptic conditions for 12–24 h. Following incubation, 0.1 mL of the inoculum was extracted from each broth concentration and introduced onto the MHA medium to observe the MIC. The plates were incubated for 24 h. The MIC refers to the drug concentration at which either no visible growth or less than three colonies are observed on the plates. In this context, the absence of visible growth or minimal colony formation indicates an inhibition activity of 99% or 100%, respectively [15].

2.7.3 Antioxidant activity assay

The potential of AgNPs derived from *S. aromaticum* for their scavenging activity against free radicals, specifically the DPPH radical was determined. The experimental procedure employed in this research was based on the methodology described by Giriwono et al. [16], with slight modifications [17]. The antioxidant activity of aqueous extracts was determined using the DPPH assay. A methanolic solution of

DPPH at a concentration of 0.1 mM was prepared. Subsequently, 0.5 mL of this DPPH solution was combined with 0.5 mL of clove aqueous extracts. The concentration of the aqueous extract ranged from 25 to 500 g·mL⁻¹. This experimental setup allowed us to evaluate the potential antioxidant properties of the aqueous extracts. The testing procedure was replicated three times for Sa-AgNPs and the aqueous extract. This study utilized the absence of DPPH in methanol as the blank, while ascorbic acid was employed as the standard. The control group consisted of DPPH dissolved in methanol without the inclusion of any samples. The reaction mixture was allowed to stand undisturbed for 30 min in a light-free environment. Subsequently, the absorbance at a wavelength of 520 nm was determined using a UV-Vis spectrophotometer. The percentage of scavenging was calculated using the following formula:

Free radical scavenging activity(%)
$$= \frac{\text{Control Abs} - \text{Test sample(Abs)}}{\text{Control(Abs)}} \times 100$$

2.7.4 MTT assay

The MTT assay was used to test the cytotoxicity of Sa-AgNPs. The human fibroblast cell line L929 was used to test the cytotoxic effect of the biosynthesized Sa-AgNPs. The MTT assay involves the reduction of tetrazolium components by viable cells, resulting in the formation of purple-colored crystals. The stock solution of the samples was prepared at 1 mg·mL⁻¹ and then diluted with the cell culture medium to achieve the desired concentrations of 5, 10, 25, 50, and 100 µg·mL⁻¹. The compound was introduced at varying concentrations and subsequently incubated with cells suspended in DMSO upon reaching 90% confluency. The negative control in this experiment consisted of cells cultured in a compound-free medium, while the positive control involved treating the cells with Triton X-100 for 48 h. A solution of MTT was prepared by dissolving 5 mg of the substance in 1 mL of DMSO and subjecting it to filter sterilization. Ten microliters of the MTT solution were additionally dilution with 90 µL of serum and phenol red-free medium, resulting in a final volume of 100 µL. Each well was treated with 100 µL of a solubilization solution consisting of 10% Triton X-100, 0.1 N HCl, and isopropanol. The mixture was then incubated at room temperature for 1 h to facilitate the dissolution of the development of crystals. The solution's absorbance was quantified at a wavelength of 570 nm utilizing a Robonik Elisa plate reader (Read well TOUCH model). Each experiment was analyzed using three replicate samples [18].

2.8 Statistical analysis

All the experiments were performed in triplicate. The data were recorded as mean \pm standard deviation from three separate trials.

2.9 Results and discussion

In this study, UV-Vis spectroscopy was used to confirm the presence of AgNPs in an aqueous extract of *S. aromaticum* and determine their stability. The experimental results depicted in Figure 1a provide evidence for the formation and enduring nature of AgNPs.

The initial indication of the successful shape of AgNPs is observed, as evidenced by the change in color from pale brown to dark brown. In this study, an aqueous extract of

S. aromaticum was employed as a reducing agent to synthesize AgNPs by reducing AgNO₃. The appearance of a dark brown color can be attributed to several factors, including the dimensions of the particles, their ability to absorb visible light strongly, and the activation of surface plasmon resonance. The UV-visible spectrum of synthesized AgNPs was examined to investigate their optical properties. The analysis revealed the presence of a distinct absorbance band peak in the range of 420–470 nm, which indicates surface plasmon resonance. The observation of a redshift in the absorbance peak indicates the progressive growth of nanoparticles from smaller to larger sizes.

Standardizing and optimizing silver nanoparticle synthesis involves altering different pH values, metal ion concentrations, and substrate concentrations. It was revealed that these factors substantially impacted the control of the form and size of AgNPs. In contrast to essential media, the particle size is anticipated to be more noticeable in an acidic

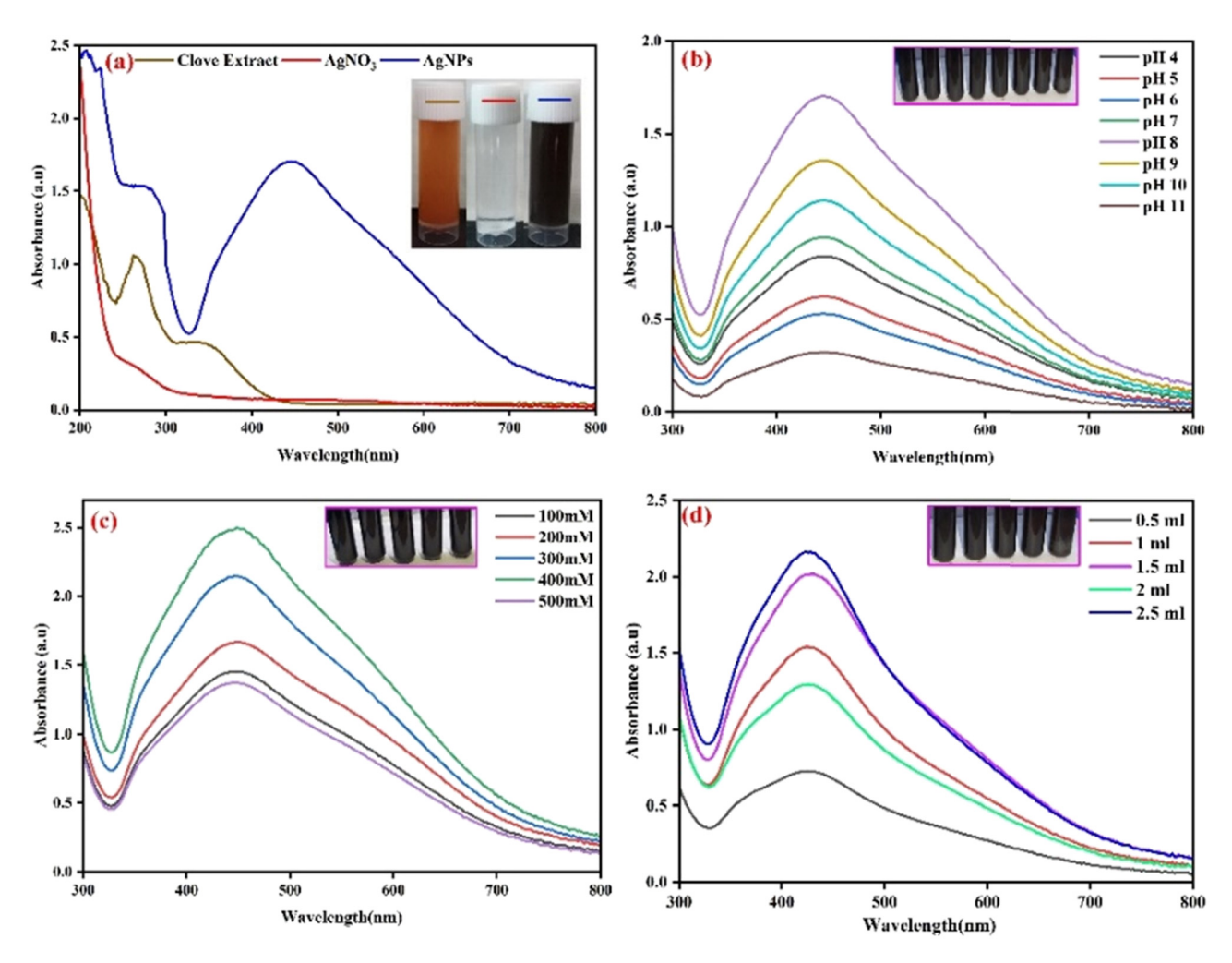


Figure 1: UV-Vis spectra of the extract, silver ions, and AgNPs (Inset: The solution of the extract, silver ions, and AgNPs) (a), pH (b), metal ions (c), and the extract concentration (d) optimization.

medium [19]. AgNPs were formed at pH 8 and distributed in a monodispersed state without aggregating. This was substantiated by the absorbance peaks at 440 nm, which were further validated by the UV-Vis spectrum data, as seen in Figure 1b. The pH impact on the size effect is shown in colors ranging from pale brown to dark brown [20]. Figure 1c shows that a 400 mM metal ion concentration was the optimum for production. This remark suggests that a considerable increase in the concentration of metal ions stimulates more remarkable synthesis. According to absorption spectra, 2.5 mL of the *S. aromaticum* aqueous extract in AgNO₃ solution was the ideal substrate concentration for producing AgNPs, and increasing the substrate concentration resulted in maximum synthesis (Figure 1d).

The TEM images in Figure 2a show uniform particle distribution, but their shapes vary based on the concentration of $AgNO_3$ used.

At increased concentrations of AgNO₃ examined, the particles displayed polydispersity, manifesting as various

shapes, including spherical, triangular, and hexagonal forms and irregular structures. In contrast, at the lowest concentration investigated, the particles were predominantly observed to be spherical. TEM analysis was crucial in determining the sizes and shapes of the synthesized nanoparticles. The EDX spectrum in Figure 2b reveals a prominent peak at 3 keV, providing evidence of silver (Ag) and the organic constituents that coat the silver aggregates. These organic components include carbon (C), chlorine (Cl), and copper (Cu) atoms, as reported by Bello et al. [21]. The presence of silver (Ag) can be attributed to the formation of AgNPs.

On the other hand, the aqueous extract of *S. aromaticum* and the carbon-coated grid used to prepare the sample are attributed to the presence of carbon (C), chlorine (Cl), and copper (Cu) atoms. The spectral analysis also verified that AgNPs exist in a metallic state, devoid of any silver oxide formation and devoid of any additional impurities. Furthermore, the XRD pattern obtained from the biosynthesis of Sa-AgNPs using the plant clove aqueous extract

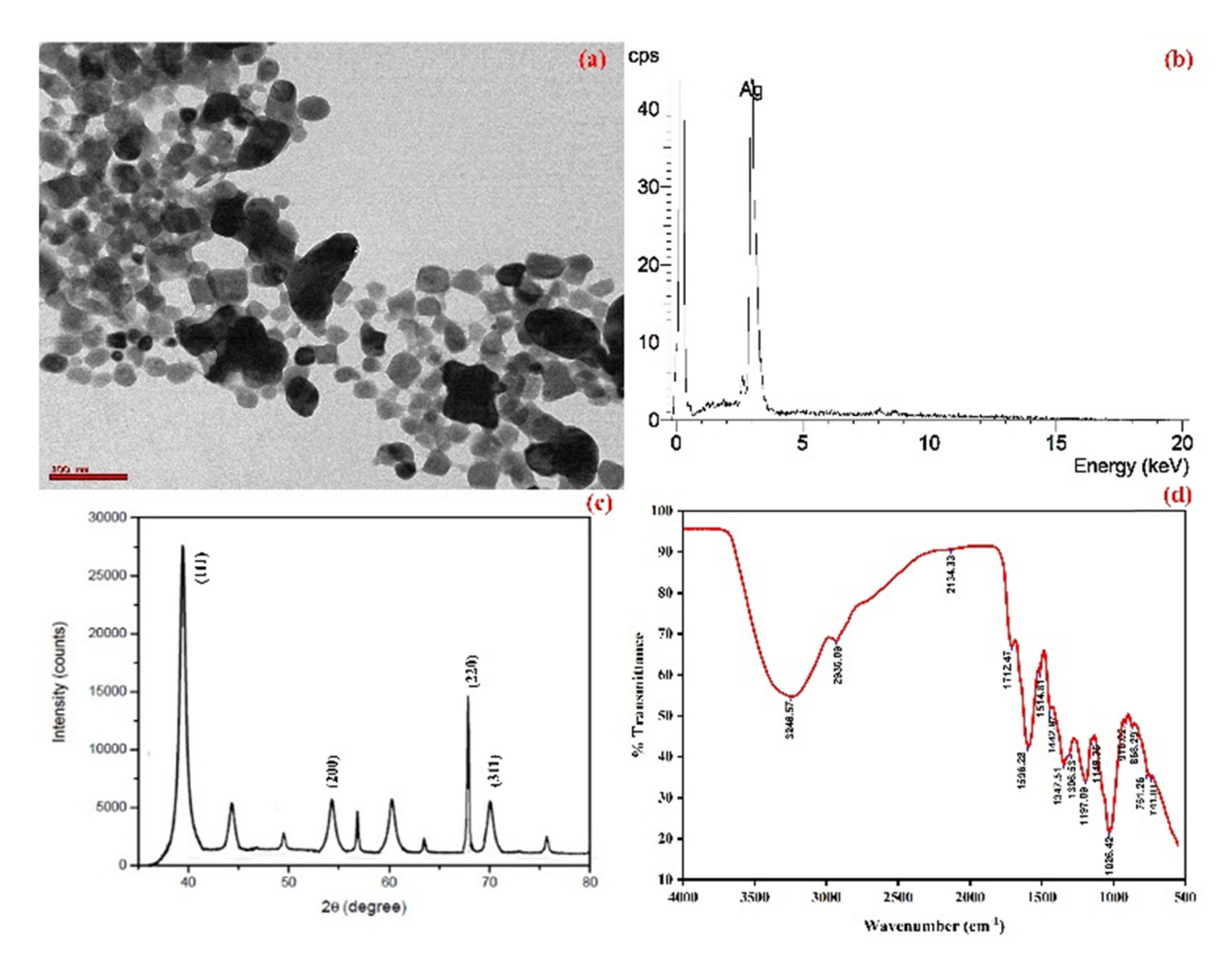


Figure 2: HR-TEM image (a), EDS mapping (b), XRD pattern (c), and FTIR spectrum (d) of Sa-AgNPs.

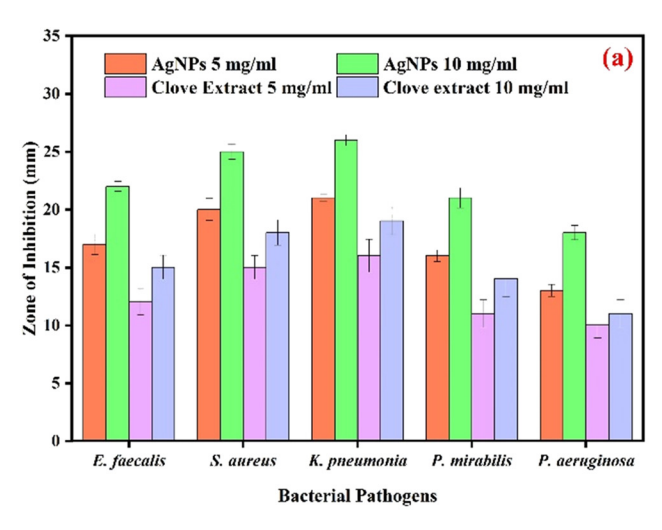
revealed a crystalline structure with a face-centered cubic (fcc) arrangement. Figure 2c exhibits a distinct pattern consisting of four different diffraction peaks observed at 41.21, 55.68, 68.42, and 71.32°, which correspond to the lattice plane values of (111), (200), (220), and (311) for silver crystals, respectively. The size of the synthesized product was observed to be in the nanometer range, explicitly ranging from 10 to 36 nm [22–26].

An FTIR analysis was conducted to determine possible functional groups in Sa-AgNPs that were obtained. The FTIR spectra of AgNPs are depicted in Figure 2d, and the presence of hydrogen-bonded N-H stretching aliphatic primary amine groups is indicated by the prominent and broad peak observed at 3,246 cm⁻¹ [27,28]. The observed peaks at 2,963 and 2,134 cm⁻¹ could be attributed to the medium C-H stretching alkane and strong N=N=N stretching azide functional groups. The spectral regions at 1,712, 1,596, 1,514, 1,442, and 1,347 cm⁻¹ correspond to the strong C=O stretching carboxylic acid dimer, medium N-H bending amine, N-O stretching nitro compound, medium C-H alkane methyl group, and O-H bending alcohol, respectively. Based on the findings of a prior investigation, it was observed that the band was detected within the spectral range of 1,306, 1,197, 1,149, and 1,026 cm⁻¹, suggesting the presence of an S=0 stretching sulfone and C-N stretching amine [29]. The observed peak at a wavenumber of 916 cm⁻¹ may indicate the strong C=C bending associated with an alkene. According to Raghu et al. [27], the peak observed at a wavenumber of 868 cm⁻¹ can be attributed to the strong C–Cl stretching halo compound. The observed peak at wavenumbers of 761 and 741 cm⁻¹ is ascribed to the strong C=C bending alkene functional groups. The observations mentioned above have confirmed the presence of various functional groups that

potentially serve as both reducing and stabilizing agents in the AgNP synthesis [30].

The biological activity of inorganic nanoparticles is influenced by several key factors, including size distribution, morphology, surface charge, surface chemistry, and the presence of capping agents. These factors play a crucial role in determining the interaction of nanoparticles with biological systems, affecting their therapeutic or functional efficacy.

- Size distribution: The size of nanoparticles has a significant impact on their biological activity. Studies have shown that nanoparticles with specific size ranges exhibit enhanced cellular uptake, improved drug delivery capabilities, and altered biodistribution patterns [31]. This is attributed to the fact that smaller nanoparticles can more easily penetrate cellular barriers.
- 2. Morphology: The shape and morphology of nanoparticles can influence their biological behavior. For instance, studies have demonstrated that different shapes (e.g., spheres, rods, or cubes) can lead to varying cellular responses and biodistribution patterns [32,33]. This is likely due to differences in surface area, surface energy, and ligand presentation.
- 3. Surface charge: The surface charge of nanoparticles, determined by the presence of functional groups or charge-bearing ligands, can affect their interactions with biological molecules and cells. Positively charged nanoparticles may exhibit enhanced cellular internalization, while negatively charged ones may have improved stability in physiological environments [34].
- 4. Surface chemistry: The chemical composition of the nanoparticle surface plays a crucial role in its biological activity. Functional groups or ligands on the surface can mediate specific interactions with biological molecules



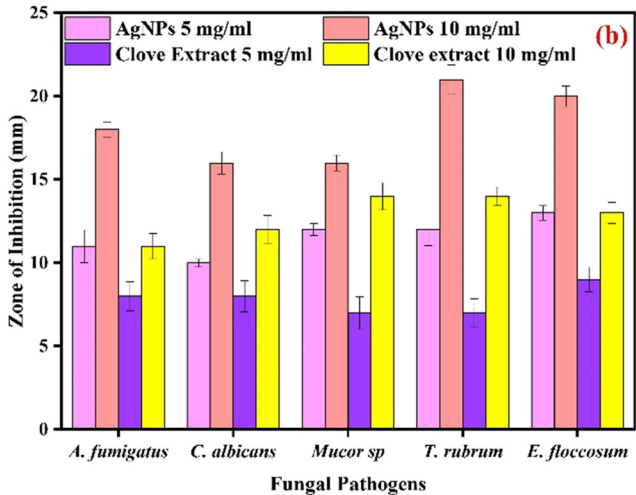


Figure 3: Antibacterial (a) and antifungal (b) activity of the clove extract and Sa-AgNPs.

or cells. For example, surface modifications with targeting ligands can enhance the specificity of nanoparticles for certain cell types [35].

5. Capping agents: Capping agents, which are often used in nanoparticle synthesis to stabilize and control their growth, can also influence biological activity. They form a protective layer around the nanoparticle, affecting its surface properties and interactions with biological systems [36]. Studies have shown that the choice of the capping agent can impact cellular uptake and cytotoxicity of nanoparticles [37]. These factors collectively contribute to the biological behavior of inorganic nanoparticles and are essential considerations in the design and development of nanomaterials for various applications, including drug delivery, imaging, and diagnostics.

The results of antibacterial activity demonstrate a significant decrease in growth after the incubation period on plates at Sa-AgNPs and clove aqueous extract concentrations of 5 and 10 mg·mL⁻¹, respectively, as depicted in Figure 3a.

The observed inhibition of bacterial proliferation in the vicinity of the well can be attributed to diffusion, whereby inhibitory compounds are dispersed. K. pneumoniae demonstrated the most significant zone of inhibition $(26 \pm 0.48 \,\mathrm{mm})$, followed by S. aureus $(25 \pm 0.67 \,\mathrm{mm})$, E. faecalis (22 \pm 0.43 mm), P. mirabilis (21 \pm 0.89 mm), and P. aeruginosa (18 \pm 0.62 mm) at the highest concentration (10 mg·mL⁻¹) of synthesized Sa-AgNPs. Bacteria exposure to Sa-AgNPs has been shown to result in cell death due to the disruption of the cytoplasmic membrane and substantial leakage of various biomolecules (amino acids, proteins, carbohydrates, and nucleotides). The efficacy of Sa-AgNPs and the aqueous extract against the tested pathogens was determined by measuring the MIC. The results indicated that these substances were effective against various microorganisms (Table 1).

According to Suhas et al. [28], the high conductivity of cells treated with Sa-AgNPs is due to the expulsion of

Table 1: MIC values of the *S. aromaticum* extract and synthesized Sa-AgNPs against bacterial pathogens

Bacterial strain	MIC (mg·mL ^{−1})		Tetracycline
	Sa-AgNPs	Clove aqueous extract	(µg·mL ^{−1})
E. faecalis	0.78	3.125	0.8
S. aureus	0.78	3.125	0.8
K. pneumonia	0.78	3.125	1.6
P. mirabilis	1.56	12.5	3.2
P. aeruginosa	1.56	12.5	1.6

cellular components from the cell. Ag⁺ has been suggested by some researchers to interact with disulfide or sulfhydryl groups of enzymes, leading to the perturbation of metabolic processes and, as a result, cell lysis. Studies reveal that they can infiltrate into the cells, hinder the replication of DNA, and impede the proliferation of microbes [38,39].

In antifungal activity, maximum inhibition was found to be against T. rubrum (21 \pm 0.89 mm), followed by E. floccosum (20 \pm 0.62 mm), A. fumigatus (18 \pm 0.43 mm), C. albicans (16 \pm 0.67 mm), and Mucor sp. (16 \pm 0.48 mm) at the higher concentration of AgNPs (10 mg·mL⁻¹) (Figure 3b). Jo et al. [40] reported a great potential of Sa-AgNPs in controlling spore-producing fungal plant pathogens and that these nanoparticles may be less toxic than synthetic fungicides [40]. The attachment of AgNPs to the fungal cell membrane and their subsequent entrance into the fungi are followed by functional changes in the sequence of cellular respiratory reactions and, ultimately, cell death [41]. The observed fungicidal activity was speculated to be due to the inactivation of sulfhydryl groups in the fungal cell wall, substantial formation of insoluble compounds, and disruption of membrane-bound enzymes and lipids, leading to cell death [42].

Sa-AgNPs use phytochemicals like terpenoids, flavonoids, phenols, and other phytoconstituents as a capping agent to get rid of DPPH radicals. The uptake of hydrogen enables the DPPH solution to become yellow after being exposed to nanoparticles [43]. The synthesized Sa-AgNPs and aqueous extract capacity to scavenge DPPH is on par with ascorbic acid. The findings show that Sa-AgNPs had the highest scavenging efficiency, with a value of 79.98%, at their maximum concentration of 500 g·mL⁻¹. At the exact dosage, the plant extract and ascorbic acid both demonstrated scavenging potentials of 70.43% and 92.86%, respectively (Figure 4). It was determined that the IC₅₀ values for AgNPs and the plant extract were 286.56 and 427.53 g·mL⁻¹, respectively. The IC₅₀ value for quercetin was determined to be 124 g·mL⁻¹. Our findings are consistent with previous findings on the ecological synthesis of AgNPs using the Lippia nodiflora aerial extract. They discovered that the DPPH scavenging capacity increased proportionately with the sample concentration. At a concentration of 500 g·mL $^{-1}$, Sa-AgNPs exhibited the most excellent scavenging activity of 67%, while the standard exhibited 83% scavenging activity [44].

The research findings demonstrated a significant positive association between the concentration of Sa-AgNPs and the observed cytotoxic effects. The proliferation of cells was hindered by Sa-AgNPs at different concentrations of 5, 10, 25, 50, and 100 μ g·mL⁻¹, leading to corresponding decreases of 4.78%, 8.33%, 12.77%, 17.64%, and 20.88%, as illustrated in Figure 5.

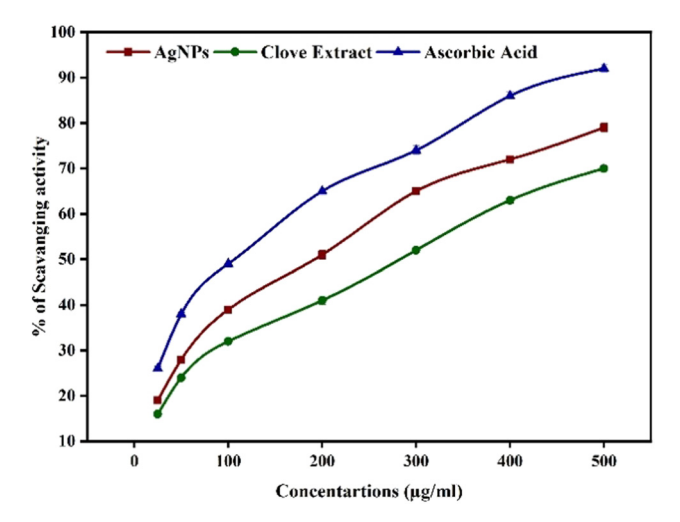


Figure 4: Percentage scavenging values of synthesized Sa-AgNPs, clove extract, and ascorbic acid in DPPH.

Hence, the biological synthesis of Sa-AgNPs resulted in a cytotoxic response in the targeted cells, which allowed for the determination of the inhibitory concentration (IC $_{50}$) at 48 μ g·mL $^{-1}$ after a 24 h incubation [45]. On the other hand, the cells treated with Sa-AgNPs displayed distinct morphological changes, including retraction, rounding, detachment from the surface, and the accumulation of suspended cells. The results of this study suggest that the utilization of Sa-AgNPs can result in the initiation of apoptosis in human fibroblast cells (L929), aligning with prior research.

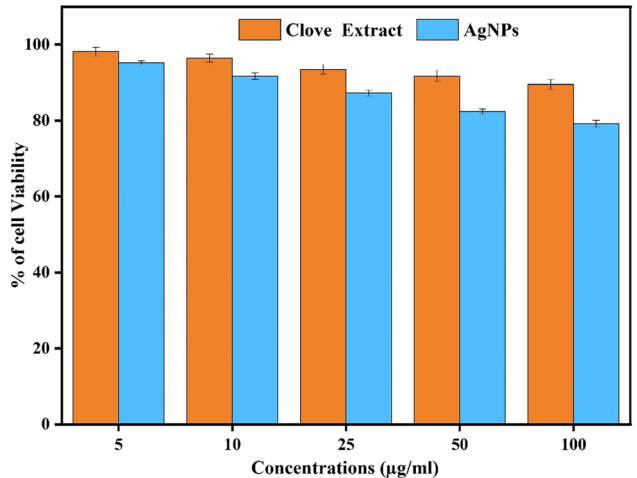


Figure 5: Cytotoxic effect of the extract and Sa-AgNPs on human fibroblast cells (L929). Significantly different (p < 0.05) compared in each assay.

2.10 Antibacterial, antifungal, and antioxidant mechanisms

The antibacterial, antifungal, and antioxidant mechanisms of action of *S. aromaticum*-mediated synthesis of Sa-AgNPs need to be fully understood. It involves many different pathways (Figure 6).

A possible mechanism is that the Sa-AgNPs can disrupt the bacteria and fungi cell membranes, leading to cell

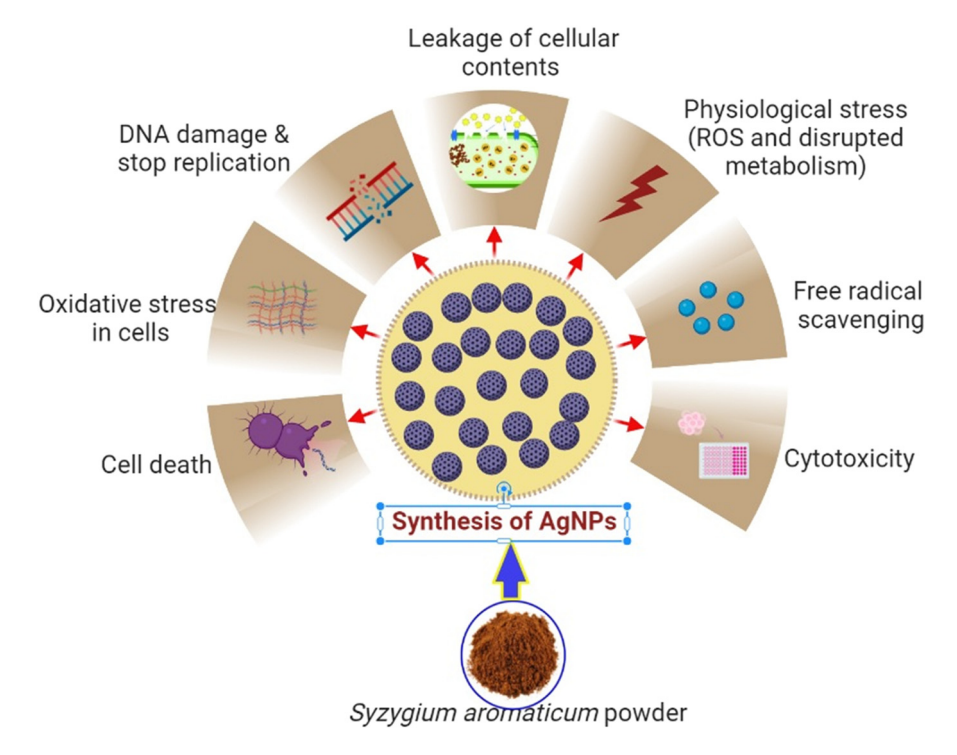


Figure 6: Possible antibacterial, antifungal, and cytotoxic effects of Sa-AgNPs.

death [46,47]. Sa-AgNPs can also bind to the DNA of bacteria and fungi, preventing them from replicating. In addition, Sa-AgNPs can generate reactive oxygen species (ROS), damaging bacteria and fungi cells. ROS can also cause oxidative stress in cells, leading to cell death [48]. Finally, Sa-AgNPs have been shown to have antioxidant properties, which can protect cells from damage caused by free radicals. This antioxidant activity may help protect cells from the toxicity of Sa-AgNPs [49,50]. Overall, the antibacterial, antifungal, and antioxidant mechanisms of action of Sa-AgNPs are complex and need to be fully understood. However, it involves several pathways, including disruption of cell membranes, DNA binding, ROS generation, and antioxidant activity [51]. Here are some specific examples of how Sa-AgNPs can exert their antibacterial, antifungal, and antioxidant effects:

- Antibacterial activity: Sa-AgNPs are effective against many bacteria, including *S. aureus*, *E. coli*, *P. aeruginosa*, and *S. typhimurium*. Sa-AgNPs can kill bacteria by disrupting their cell membranes, which can lead to the leakage of cellular contents and cell death.
- Antifungal activity: Sa-AgNPs have also been effective against various fungi, including *C. albicans*, *A. fumigatus*, and *T. rubrum*. Sa-AgNPs can kill fungi by damaging their cell walls, leading to cell death.
- Antioxidant activity: Studies have shown that Sa-AgNPs have antioxidant properties that shield cells from free radical damage. Free radicals are unstable molecules that can damage cells by reacting with DNA, proteins, and lipids. Sa-AgNPs can scavenge free radicals, preventing them from causing damage to cells.

The antibacterial, antifungal, and antioxidant properties of Sa-AgNPs make them a potential candidate for several applications, including in medicine, water purification, and food preservation. However, further research is needed to understand the mechanism of action of Sa-AgNPs fully and to assess their safety and efficacy.

3 Conclusion

The results of this study show that Sa-AgNPs can be made in a way that is cheap and good for the environment by using *S. aromaticum* buds as both a capping agent and a reducing agent. The visual confirmation of color formation was used to verify the successful synthesis of Sa-AgNPs. The XRD analysis indicated the presence of a crystal structure, with the observed grain size ranging from 10 to 36 nm of synthesized Sa-AgNPs. The TEM-EDX images showed a lot of clumping around the nanoparticles, possibly due to the accumulation of plant materials. The strong signals of

the silver element and the lack of any noticeable impurities confirmed it. FTIR analysis showed that the synthesized Sa-AgNPs had organic compounds with functional groups that came from the buds of S. aromaticum. The synthesis of Sa-AgNPs with a nano-size was further validated through morphology and structural analysis. Sa-AgNPs exhibited greater efficacy in inhibiting the growth of bacteria and fungi compared to the aqueous extract. Also, different methods, such as the DPPH radical scavenging assay, were used to test how well green-synthesized Sa-AgNPs got rid of free radicals. The outcomes were compared to those of the well-known ascorbic acid. It was revealed that the dosage affected the scavenging ability of the standard, seed extract, and Sa-AgNPs. When delivered at lower doses (5 g·mL⁻¹), the Sa-AgNPs created using the S. aromaticum aqueous extract had a cytotoxicity of up to 95.22%. Additionally, in vivo tests are necessary to determine this nanomedicine's effectiveness in cancer treatment.

Acknowledgement: The authors thank the Researchers Supporting Project (number RSP2023R114), King Saud University, Riyadh, Saudi Arabia, for the financial support.

Funding information: This research was funded by King Saud University Researchers Supporting Project (no. RSP2023R114), King Saud University, Riyadh, Saudi Arabia.

Author contributions: Moorthy Muruganandham: performed experiments and writing – original draft; Fatimah Oleyan Al-Otibi: writing – review and editing and formal analysis; Raedah Ibrahim Alharbi and Kanagasabapathy Sivasubramanian: writing – review and editing, visualization, and investigation; Ramalingam Karthik Raja and Palanivel Velmurugan: writing – review and editing, resources, and investigation; Palanivel Velmurugan: conceptualization, methodology, funding acquisition, and writing – review and editing.

Conflict of interest: The authors state no conflict of interest.

Data availability statement: All data generated or analyzed during this study are included in this published article.

References

- [1] Van Dijken A, Meulenkamp EA, Vanmaekelbergh D, Meijerink A. Identification of the transition responsible for the visible emission in ZnO using quantum size effects. J Lumin. 2000;90(3–4):123–8.
- [2] Singhal G, Bhavesh R, Sharma AR, Singh RP. Eco-friendly biosynthesis of gold nanoparticles using medicinally important Ocimum basilicum leaf extract. Adv Sci Eng Med. 2012;4(1):62–6.

DE GRUYTER

- [3] Andersson M, Pedersen JS, Palmqvist AEC. Silver nanoparticle formation in microemulsions acts as a template and a reducing agent. Langmuir. 2005;21(24):11387–96.
- [4] Chandran SP, Chaudhary M, Pasricha R, Ahmad A, Sastry M. Synthesis of gold nanotriangles and silver nanoparticles using Aloe vera plant extract. Biotechnol Prog. 2006;22(2):577–83.
- [5] Vishwanath R, Negi B. Conventional and green methods of synthesis of silver nanoparticles and their antimicrobial properties. Curr Res Green Sustain Chem. 2021;4:100205.
- [6] Vidya C, Hirematha S, Chandraprabha MN, Antonyraj ML, Gopala IV, Jaina A, et al. Green synthesis of ZnO nanoparticles by Calotropis gigantea. Int J Curr Eng Technol. 2013;1(1):118–20.
- [7] Ahmed S, Ahmad M, Swami BL, Ikram S. Green synthesis of silver nanoparticles using *Azadirachta indica* aqueous leaf extract. J Radiat Res Appl Sci. 2016 1;9(1):1–7.
- [8] Aruna A, Nandhini R, Karthikeyan V, Bose P. Synthesis and characterization of silver nanoparticles of insulin plant (*Costus pictus* D. Don) leaves. Asian J Biomed Pharm Sci. 2014;4(34):1–6.
- [9] Ahmed S, Ahmad M, Swami BL, Ikram S. A review on plant extract mediated synthesis of silver nanoparticles for antimicrobial applications: green expertise. J Adv Res. 2016;7(1):17–28.
- [10] El-Khawaga AM, Zidan A, Abd El-Mageed AI. Preparation methods of different nanomaterials for various potential applications: A review. J Mol Struct. 2023;1281:135148.
- [11] Vijayaraghavan K, Nalini SK, Prakash NU, Madhankumar DJ. Biomimetic synthesis of silver nanoparticles by aqueous extract of Syzyqium aromaticum. Mater Lett. 2012;75:33–5.
- [12] Khan MA, Khan T, Nadhman A. Applications of plant terpenoids in the synthesis of colloidal silver nanoparticles. Adv Colloid Interface Sci. 2016;234:132–41.
- [13] Lakhan MN, Chen R, Shar AH, Chand K, Shah AH, Ahmed M, et al. Eco-friendly green synthesis of clove buds extract functionalized silver nanoparticles and evaluation of antibacterial and antidiatom activity. J Microbiol Methods. 2020;173(105934):1–9.
- [14] Satyavani K, Gurudeeban S, Ramanathan T, Balasubramanian T. Toxicity study of silver nanoparticles synthesized from *Suaeda monoica* on Hep-2 cell line. Avicenna J Med Biotechnol. 2012;4(1):35–9.
- [15] Indumathi T, Theivarasu C, Pradeep I, Rani MT, Magesh G, Rahale CS, et al. Effects of Nd doping on structural, optical, morphological and surface-chemical state analysis of ZnO nanoparticles for antimicrobial and anticancer activities. Surf Interfaces. 2021;23(101000):1–10.
- [16] Giriwono PE, Iskandriati D, Tan CP, Andarwulan N. In-vitro antiinflammatory activity, free radical (DPPH) scavenging, and ferric reducing ability (FRAP) of Sargassum cristaefolium lipid-soluble fraction and putative identification of bioactive compounds using UHPLC-ESI-ORBITRAP-MS/MS. Food Res Int. 2020;137(109702):1–10.
- [17] Sobiyana P, Anburaj G, Marimuthu M, Manikandan R. Phytochemical analysis and in vitro antibacterial activity of *Tabebuia arg entea*. J Pharmacogn Phytochem. 2019;8(1):1226–9.
- [18] Kandasamy S, Narayanan V, Sumathi S, Manikandan R. Zinc and manganese substituted hydroxyapatite/CMC/PVP electrospun composite for bone repair applications. Int J Biol Macromol. 2020:145:145–30
- [19] Khalil MM, Ismail EH, El-Baghdady KZ, Mohamed D. Green synthesis of silver nanoparticles using olive leaf extract and its antibacterial activity. Arab J Chem. 2014;7(6):1131–9.

- [20] Gontijo LA, Raphael E, Ferrari DP, Ferrari JL, Lyon JP, Schiavon MA. pH effect on the synthesis of different size silver nanoparticles evaluated by DLS and their size-dependent antimicrobial activity. Rev Mater. 2020;25(4):1–10.
- [21] Bello BA, Khan SA, Khan JA, Syed FQ, Mirza MB, Shah L, et al. Anticancer, antibacterial and pollutant degradation potential of silver nanoparticles from *Hyphaene thebaica*. Biochem Biophys Res Commun. 2017;490(3):889–94.
- [22] Hamedi S, Shojaosadati SA, Mohammadi A. Evaluation of the catalytic, antibacterial and anti-biofilm activities of the *Convolvulus arvensis* extract functionalized silver nanoparticles. J Photochem Photobiol B Biol. 2017;167:36–44.
- [23] Kumar DA, Palanichamy V, Roopan SM. Green synthesis of silver nanoparticles using Alternanthera dentata leaf extract at room temperature and their antimicrobial activity. Spectrochim Acta A Mol Biomol Spectrosc. 2014;127:168–71.
- [24] Kumar PV, Pammi SV, Kollu P, Satyanarayana KV, Shameem U. Green synthesis and characterization of silver nanoparticles using Boerhaavia diffusa plant extract and their antibacterial activity. Ind Crop Prod. 2014;52:562–6.
- [25] Raj S, Mali SC, Trivedi R. Green synthesis and characterization of silver nanoparticles using *Enicostemma axillare* (Lam.) leaf extract. Biochem Biophys Res Commun. 2018;503(4):2814–9.
- [26] Ibrahim HM. Green synthesis and characterization of silver nanoparticles using banana peel extract and their antimicrobial activity against representative microorganisms. J Radiat Res Appl Sci. 2015;8(3):265–75.
- [27] Raghu AV, Gadaginamath GS, Priya M, Seema P, Jeong HM, Aminabhavi TM. Synthesis and characterization of novel polyurethanes based on N1, N4-bis [(4-hydroxyphenyl) methylene] succinohydrazide hard segment. J Appl Polym Sci. 2008;110(4):2315–20.
- [28] Suhas DP, Jeong HM, Aminabhavi TM, Raghu AV. Preparation and characterization of novel polyurethanes containing 4,4′-{oxy-1,4-diphenyl bis(nitromethylidine)}diphenol schiff base diol. Polym Eng Sci. 2014;54(1):24–32.
- [29] Sathishkumar P, Preethi J, Vijayan R, Yusoff AR, Ameen F, Suresh S, et al. Anti-acne, anti-dandruff and anti-breast cancer efficacy of green synthesised silver nanoparticles using *Coriandrum sativum* leaf extract. J Photochem Photobiol B Biol. 2016;163:69–76.
- [30] Harshiny M, Matheswaran M, Arthanareeswaran G, Kumaran S, Rajasree S. Enhancement of antibacterial properties of silver nanoparticles-ceftriaxone conjugate through Mukia maderaspatana leaf extract mediated synthesis. Ecotoxicol Environ Saf. 2015;121:135–41.
- [31] Barabadi H, Hosseini O, Jounaki K, Sadeghian-Abadi S, Ashouri F, Alrikabi AMA, et al. Bioinspired green-synthesized silver nanoparticles: *In vitro* physicochemical, antibacterial, biofilm inhibitory, genotoxicity, antidiabetic, antioxidant, and anticoagulant performance. Mater Adv. 2023;4(14):3037–54.
- [32] Yaqub A, Rashid M, Ditta SA, Malkani N, Ali NM, Yousaf MZ, et al. In vivo antioxidant potential of biogenic silver nanoparticles synthesized from Psidium guajava L. Nano Biomed Eng. 2023;15(3):225–38. doi: 10.26599/NBE.2023.9290026.
- [33] Albanese A, Tang PS, Chan WC. The effect of nanoparticle size, shape, and surface chemistry on biological systems. Annu Rev Biomed Eng. 2012;14:1–16.
- [34] Saravanan M, Barabadi H, Vahidi H, Webster TJ, Medina-Cruz D, Mostafavi E, et al. Emerging theranostic silver and gold nanobiomaterials for breast cancer: present status and future prospects.

- In: Anand K, Saravanan M, Chandrasekaran B, Kanchi S, Panchu SJ, Chen Q, editors. Handbook on Nanobiomaterials for Therapeutics and Diagnostic Applications. Amsterdam: Elsevier; 2021. p. 439–56.
- [35] Barabadi H, Webster TJ, Vahidi H, Sabori H, Kamali KD, Shoushtari FJ, et al. Green nanotechnology-based gold nanomaterials for hepatic cancer therapeutics: a systematic review. Iran J Pharm Res: IJPR. 2020;19(3):3.
- [36] Nemati M, Bani F, Sepasi T, Zamiri RE, Rasmi Y, Kahroba H, et al. Unraveling the effect of breast cancer patients' plasma on the targeting ability of folic acid-modified chitosan nanoparticles. Mol Pharm. 2021;18(12):4341–53.
- [37] Mahmoudi M, Serpooshan V. Silver-coated engineered magnetic nanoparticles are promising for the success in the fight against antibacterial resistance threat. ACS Nano. 2012;6(3):2656–64.
- [38] Raja S, Ramesh V, Thivaharan V. Green biosynthesis of silver nanoparticles using Calliandra haematocephala leaf extract, their antibacterial activity and hydrogen peroxide sensing capability. Arab J Chem. 2017;10(2):253–61.
- [39] Nel AE, M\u00e4dler L, Velegol D, Xia T, Hoek EM, Somasundaran P, et al. Understanding biophysicochemical interactions at the nano-bio interface. Nat Mater. 2009;8(7):543-57.
- [40] Jo YK, Kim BH, Jung G. Antifungal activity of silver ions and nanoparticles on phytopathogenic fungi. Plant Dis. 2009;93(10):1037–43.
- [41] Prabhu S, Poulose EK. Silver nanoparticles: mechanism of antimicrobial action, synthesis, medical applications, and toxicity effects. Int Nano Lett. 2012;2(32):1–10.
- [42] Jaidev LR, Narasimha G. Fungal mediated biosynthesis of silver nanoparticles, characterization and antimicrobial activity. Colloids Surf B. 2010;81(2):430–3.
- [43] Guntur SR, Kumar NS, Hegde MM, Dirisala VR. In vitro studies of the antimicrobial and free-radical scavenging potentials of silver nanoparticles biosynthesized from the extract of *Desmostachya bipinnate*. Anal Chem Insights. 2018;13:1–9.

- [44] Sudha A, Jeyakanthan J, Srinivasan P. Green synthesis of silver nanoparticles using *Lippia nodiflora* aerial extract and evaluating their antioxidant, antibacterial and cytotoxic effects. Resource-Efficient Technol. 2017;3(4):506–15.
- [45] Abdal Dayem A, Hossain MK, Lee SB, Kim K, Saha SK, Yang GM, et al. The role of reactive oxygen species (ROS) in the biological activities of metallic nanoparticles. Int J Mol Sci. 2017;18(1):1–21.
- [46] Saravanan M, Barabadi H, Vahidi H. Green nanotechnology: isolation of bioactive molecules and modified approach of biosynthesis. In: Biogenic Nanoparticles for Cancer Theranostics. Amsterdam: Elsevier; 2021. p. 101–22.
- [47] Barabadi H, Mohammadzadeh A, Vahidi H, Rashedi M, Saravanan M, Talank N, et al. *Penicillium chrysogenum*-derived silver nanoparticles: exploration of their antibacterial and biofilm inhibitory activity against the standard and pathogenic *Acinetobacter baumannii* compared to tetracycline. J Clust Sci. 2022;33(5):1929–42.
- [48] Majeed S, Saravanan M, Danish M, Zakariya NA, Ibrahim MNM, Rizvi EH, et al. Bioengineering of green-synthesized TAT peptidefunctionalized silver nanoparticles for apoptotic cell-death mediated therapy of breast adenocarcinoma. Talanta. 2023;253:124026.
- [49] Barabadi H, Vahidi H, Rashedi M, Mahjoub MA, Nanda A, Saravanan M. Recent advances in biological mediated cancer research using silver nanoparticles as a promising strategy for hepatic cancer therapeutics: a systematic review. Nanomed J. 2020;7(4):251–62.
- [50] Barabadi H, Mostafavi E, Truong LB, Cruz DM, Vahidi H, Mahjoub MA, et al. Microbial nanotechnology–based approaches for wound healing and infection control . In: Handbook of Microbial Nanotechnology. Boca Raton, Fl, USA: Academic Press; 2022. p. 1–15.
- [51] Truong LB, Cruz DM, Barabadi H, Vahidi H, Mostafavi E. Cancer therapeutics with microbial nanotechnology-based approaches. In: Handbook of Microbial Nanotechnology. Boca Raton, Fl, USA: Academic Press; 2022. p. 17–43.